

Scientific Spokesman

Wit Busza

Massachusetts Institute of
Technology-24-510
Cambridge, Massachusetts 02139
617-864-6900 ext. 7586

A STUDY OF THE AVERAGE MULTIPLICITY AND MULTIPLICITY
DISTRIBUTIONS IN HADRON-NUCLEUS COLLISIONS AT HIGH
ENERGIES

W. Busza, J.I. Friedman, H. W. Kendall and L. Rosenson
Massachusetts Institute of Technology

June, 1972

I. INTRODUCTION:

We propose to study the detailed shape of the multiplicity distribution for large values of n , and also its A -dependence in hadron-nucleus collisions at 100 and 200 GeV. Hadron-nucleon distributions will be extrapolated from the data. We further propose to compare distributions from pions, kaons and protons. Later if possible we would like to extend the measurements to higher energy.

a) Theoretical motivation:

The average number of particles produced in hadron-nucleon collisions increases logarithmically with energy. At NAL energies it is already ~ 7 . It is thus not surprising that as higher and higher energies become accessible to experimental investigation, there is more and more theoretical interest in reactions with multiparticle final states. We shall not attempt to review theoretical models of multiparticle production since there are several excellent recent review articles in the literature¹. Instead we briefly discuss characteristics of the models which motivate this proposal.

There are two categories of theoretical models of multiparticle production:

- i) models such as the particle fragmentation model, multiperipheral model, bremsstrahlung analogy model or field theoretical model which assume that the final particles are produced in a one step process,
- ii) models such as the diffraction excitation model and the one or two fireball models which assume that the multiparticle production mechanism is a two step process; first one or two compound systems are produced which then, in life-times long compared to the collision time, decay into the final multiparticle states.

All the present theoretical models have sufficient flexibility that, to the best of our knowledge, there is no one experimental measurement which can differentiate between them. In order to rule out many of the models it is necessary to study in detail various properties of multi-particle production. To illustrate this point we reproduce in table I a comparison of experimental predictions compiled by Frazer et al ¹.

From this compilation it is apparent that the average multiplicity, $\langle n \rangle$, the multiplicity distribution $P(n)$, in particular at large values of n , and partial cross-sections $\sigma(n)$ are a very useful filter. Here n is the number of particles produced in an inelastic collision and $P(n)$ is the probability of producing n particles in any one inelastic collision.

Further, Dar and Vary ² have pointed out to us that a study of the A -dependence of mean multiplicities in hadron-nucleus collisions is probably the only sensitive test which differentiates between the two general categories of theoretical models mentioned above. They point out that for category ii) the A -dependence should be energy independent whilst for category i) there should be a strong energy dependence, as illustrated in fig. 1.

b) Present knowledge of mean multiplicities and multiplicity distributions at high energy:

Figures 2 and 3 illustrate the present experimental knowledge of the mean charged multiplicities, $\langle n_{ch} \rangle$, and $P(n_{ch})$ at energies above 70 GeV. The Echo lake experiment ³ and cosmic ray emulsion exposures ⁴ have given some preliminary information on the A -dependence of $\langle n \rangle$. There is indication that $\langle n_{ch} \rangle \sim A^{0.1}$ or $A^{0.15}$. In summary, cosmic ray experiments have not yielded sufficiently accurate measurements of $\langle n_{ch} \rangle$, $P(n_{ch})$ or on the A -dependence of $\langle n_{ch} \rangle$ to differentiate between the various theoretical models.

c) The proposed experiment:

The partial cross-sections for various target materials, ranging from beryllium to uranium, will be measured at 100 GeV and 200 GeV. An extrapolation of the data to $A=1$ will yield distributions for hadron-nucleon collisions. The principle of the experimental technique proposed for the measurements is as follows:

Partially surround the target with \checkmark Cerenkov counters and measure the spectrum of pulse heights in the counter. Adequate coverage is assured with a counter array of less than 4π owing to the pronounced forward peaking in the secondaries angular distribution. For relativistic particles the number of photons per unit path length in a \checkmark Cerenkov radiator is independent of the momentum and mass of the particle, and thus the total number of photons radiated is proportional to the number of relativistic particles passing through the radiator, that is to the charged multiplicity of the interaction.

The simplicity of measurement allows data to be collected at rates greater than 10^4 interactions/sec, so that statistics are no problem in a run of even modest length, and all errors reside in systematic effects. On the other hand because of the rate at which data can be collected we feel that sufficient number of tests (e.g. runs with many target and counter thicknesses) can be performed to eliminate most of the systematic errors and obtain a reliable result. A 5% measurement of $\langle n_{ch} \rangle$ should be possible. In addition, should particle identifying \checkmark Cerenkov counters in the beam line be available at the time of measurement, we would be able to investigate whether $P(n)$ is a function of the incident particle. It will be very interesting to see if for all values of n , $P(n)$ is identical for pions, kaons and protons, as commonly believed.

Comparing this technique with bubble chamber measurements we find that because of high statistics we can study $P(n_{ch})$ for much larger value of n (up to ~ 30) and also determine the A -dependence of $\langle n_{ch} \rangle$ for a very small fraction of the machine time and without the engineering effort a bubble chamber measurement of this kind could involve. The present experiment can contribute results of importance substantially earlier than any by a high priority specially dedicated bubble chamber program.

II. Description of Experimental Method:

a) Geometry of detector:

Fig. 4 illustrates the detector arrangement. The beam is defined by two trigger counters T_1 and T_2 and by a veto counter V . The target is placed at the center of a box made of Čerenkov counters $\check{C}_1, \check{C}_3 - \check{C}_6$. Targets will range from 3 cms of Be to 0.4 mms of U.

Particles produced up to angles of 30° pass through a high quality Čerenkov counter \check{C}_1 . It consists of a polystyrene radiator (which has an optimum ratio of light output to radiation length) whose thickness is adjusted such that the path of the particle in the radiator is independent of angle and ≈ 1 cm. The intensity of Čerenkov light produced in the radiator is measured, with high efficiency, using a RCA 8854 photomultiplier as shown. Particles produced at angles of more than 30° are detected by four separate threshold Čerenkov counters $\check{C}_3 - \check{C}_6$.

\check{C}_2 is used to measure background due to high energy γ -emission from excited nuclei in the target. It also samples any particles emitted backwards in the laboratory.

b) Electronics and trigger logic:

An incident particle is defined by

- i) T_1 and T_2 both have a coincident signal of amplitude ≤ 1.5 times minimum ionizing.
- ii) No other particle in T_1 or T_2 during 10ns preceeding or 10ns following the $T_1 T_2$ signal.
- iii) No signal in V during the above 20ns interval.

These three conditions insure that only one incident particle enters the equipment during its sensitive time.

Whenever an incident particle trigger is received the pulse height of $\check{c}1$ is stored in one of the quadrants of a 1024 channel pulse height analyser. The quadrants are designated by the following conditions:

- 1: No signals in $\check{c}_3 - \check{c}_6$
- 2: signal in one of $\check{c}_3 - \check{c}_6$
- 3: signals in two of $\check{c}_3 - \check{c}_6$
- 4: signals in at least three of $\check{c}_3 - \check{c}_6$

Following a trigger the electronics is gated off for a period 10 μ sec, corresponding to the maximum dead time of the analyser.

Special runs to study very high multiplicity interactions would also be carried out; only events with large pulse heights in $\check{c}1$ would be stored.

Throughout the experiment the coincidence rate of \check{c}_2 with the beam trigger will be monitored.

The system should be capable of handling beam rates of up to 5×10^7 particles/sec and collecting data at up to 5×10^4 interactions/sec.

c) Properties of the \check{C} erenkov counters:

A crucial part of the detector system is the \check{C} erenkov counter $\check{c}1$, and it is important to consider what limitations it imposes on the measurements.

i) Minimum momentum of detected particles:

Fig. 5 shows the number of photons radiated in \check{cl} by particles of different momenta. It can be seen that \check{cl} is sensitive only for particles of $\beta > 0.7$ (e.g. $P_{\pi} \gg 140$ MeV/c). The cut-off in momentum is higher for kaons and protons however; since the major contribution to multiplicity is expected to be from pions, this should not introduce major systematic errors.

ii) Resolution:

In the range $3500 \text{ \AA} < \lambda < 5000 \text{ \AA}$ approximately 200 photons will be radiated in \check{cl} by each relativistic particle. We estimate that because of the efficient light collecting system these will give rise to ≥ 30 photoelectrons. Based on this number we estimate the resolution of \check{cl} to be as shown in fig. 6. We have included in the resolution curve the tail due to δ -rays and due to hadron interactions in the radiator. The experiment would still be feasible with a resolution worse by a factor two, as observed ⁵ in $\check{Cerenkov}$ counters with light collected in a less optimum configuration.

III. Discussion of Experimental Problems, Choice of Target Thickness, etc.

In designing the experiment we have considered the following effects which could distort the results:

- a) loss of prongs with production angle $> 30^\circ$
- b) loss of non-relativistic prongs
- c) contamination of data by high energy gamma rays from the decay of excited target nuclei.
- d) hadron showers in the target and $\check{Cerenkov}$ counters
- e) electro-magnetic showers from $\pi^0 \rightarrow 2\gamma$.
- f) distortion of pulse height spectra due to resolution of \check{cl} .

A discussion of these six effects follows:

- a) & b) Using Cocconi's ⁶ semi-empirical formula

$$\frac{d^2 N}{d p_{\perp} d p_{\parallel}} = \frac{B p_{\perp}}{b^2} e^{-p_{\parallel}/G} e^{-p_{\perp}^2/b}$$

with

$$BG = \langle \Delta^2 \rangle$$

$$BG^2 = \frac{1}{2} E_{\text{INCIDENT}}$$

$$b = 0.22 \text{ GeV}/c$$

and assuming all prongs are pions, we estimate that for

$$E_{\text{incident}} \geq 100 \text{ GeV}$$

- i) probability of losing a prong because of

$$\beta \text{ cut-off is } \leq 1.5\%$$

- ii) probability of production angle $> 30^\circ$ is $\leq 10\%$; thus with 4 counters covering angles $\geq 30^\circ$ the probability of two prongs hitting the same counter and thus being lost is $\leq 0.1\%$. In any case should this estimate be optimistic it will reflect in the $C_3 - C_6$ rates.

- c) An excited nucleus can emit a γ of energy up to $\sim 8 \text{ MeV}$ in times short compared to the resolving time of the detector. These γ 's can in principle, produce relativistic e^+e^- pairs in cl . All estimates indicate the effect to be negligible. As a precaution it will be measured using C_2^v , as described earlier.

- d) & e) Approximately one third of the particles produced will be π^0 's. These decay into 2 γ 's which can shower both in the target and in cl . In addition to the electro-magnetic showers, the produced particles can further multiply in subsequent collisions.

For these reasons it is necessary to minimize the number of collision and radiation lengths in the target and in \sqrt{cl} .

Photon statistics put a practical limit on the thickness of \sqrt{cl} at about 1 cm. polystyrene is chosen to minimize the number of radiation lengths in the radiator. The material in \sqrt{cl} dictates the minimum thickness of targets for a meaningful target-in/target-out rate. Table II lists optimum target thickness, together with estimates of contamination due to electromagnetic and hadronic showers. Most of these systematic effects can be corrected for by extrapolating to zero thickness data obtained with several targets and radiators of different thickness.

The effect of the finite resolution of \sqrt{cl} is to smear out the final spectrum. In general clear peaks at different values of n will not be visible. Fig. 7 illustrates the results that will be obtained from a 2 cms Be target if in inelastic collisions the multiplicity has a poisson distribution with $\langle n \rangle = 6$.

In every run the peaks due to uninteracted particles and pseudoelastic scatters will automatically calibrate the resolution and pulse height scale of the complete system.

Taking all the above effects into consideration we estimate that the experiment is capable of measuring the charged prong cross-section, $\sigma(n)$, to $\sim \pm 10\%$ and $\langle n_{ch} \rangle$ to $\sim \pm 5\%$. It should be noted that even prior to extrapolating the data to zero counter and target thickness, the measured $\langle n_{ch} \rangle$ will exceed the correct value by only $\sim 15\%$.

IV. Plan of Measurements and Running Time Estimates:

For the A-dependence study we plan to take data for three thicknesses each of 8 target materials (Be, C, Al, Cu, Sn, Pb, U and No-target) and each for two thicknesses of Čerenkov counter^v c1. That is a total of 48 runs at each of two energies, 100 and 200 GeV.

In order not to be limited by statistics each run should contain $\geq 10^6$ interactions, which corresponds to 10^8 incident particles for a 1% collision length target.

Beam intensities in the range $5 \times 10^4 - 5 \times 10^7$ particles/sec would be suitable for this part of the experiment. At 10^5 particles/sec a typical run would take less than 15 mins.

In addition we would like to take a few one hour runs with $\sim 10^7$ particles/sec on Be to look at distributions at very large values of n ($\lesssim 30$).

In total we request 40 hours of data taking time, 20 hours at 100 GeV and 20 hours at 200 GeV. In addition we would require about 20 hours of setting up time. Since the beam requirements are so loose, all of the setting up and probably most of the data could be taken whilst the beam itself was being set up and tested for other experiments. Before going to NAL we plan to test the technique at one of the BNL beams.

The 2.5 mr beam, where the group is participating in an already approved experiment and which offers the opportunity of using incident particle identifying Čerenkov counters^v, would probably be the most suitable location for the experiment.

If approved, we could be ready in 2 months.

References

1. W. R. Frazer et al., Rev. Mod. Phys. 44, 284 (1972); references to other comprehensive review articles on multiparticle production can be found in that paper.
2. A. Dar and J. Vary. "Method to distinguish between Multiparticle production mechanisms", to be published.
3. L. W. Jones et al, University of Michigan preprint UM-HE 71-46 (Revised) Jan., 1972.
4. Reference to cosmic ray studies of multiplicities in hadron-nucleus scattering can be found in M. Miśowicz, Progress in Elementary particles and cosmic ray physics, Vol X. 1971 p.101; also in IZ. Artykov et al NP B6, 11, 1968.
5. W. R. Ditzler and J. S. Poucher. M.I.T. internal report Nov. 1966.
6. G. Cocconi, NP B28, 341, 1971.
7. W. Galbraith et al, BNL 11598; G. Bellettini et al. NP 79, 609, 1966.
8. H. E. Bøggild et al, NP B27, 285, 1971.
9. T. Gemesi et al., paper 380 Amsterdam Conference, July 1971.
10. S. N. Gangul et al., Phys. Lett. 39B, 632, 1972. In this paper they calculate $\langle n_{\pi^{\pm}} \rangle$ from the ISR data on γ -production. When plotting thier results we assume $\langle n_{ch} \rangle = \langle n_{\pi^{\pm}} \rangle + 1.4$
11. N. A Dobrotin et al, Canadian J. of Phys. 46, S675, 1968.

FIGURE AND TABLE CAPTIONS

Table I: Comparison of experimental predictions of various theoretical models, compiled by Frazer et al (1).

Table II: Optimum thickness of targets and physical properties of target materials. Collision length calculated from inelastic proton-nucleus cross-sections (7). In calculating the additional tracks in Cl due to electro-magnetic and hadronic showers the following assumptions were made:

- i) thickness of $\overset{V}{Cl} = 1 \text{ cm}$
- ii) $\langle n_{\pi^0} \rangle = \frac{1}{2} \langle n_{ch} \rangle_{\text{primary interaction}} = 3$
- iii) $\langle n_{ch} \rangle_{\text{secondary interactions}} = 4$

Fig. 1: Dar and Vary's (2) predictions of the energy and A-dependence of the mean multiplicity in hadron-nucleus collisions, assuming the pair production mechanism is a one step process (see text). For a two step process they predict an A-dependence which is independent of energy.

Fig. 2: Compilation of data on the mean number of charged particles produced at various energies.

Fig. 3: Charged prong multiplicity distributions measured^{at} Echo lake (3) with cosmic rays of 203 Gev mean energy.

Fig. 4: Geometrical arrangement of detector system.

Fig. 5: β dependence of the photon yield in a 1cm polystyrene $\overset{V}{Cerenkov}$ detector. The curve gives the number of photons which are not absorbed in the radiator or photomultiplier windows, ie those with $3500 \text{ \AA} < \lambda < 5000 \text{ \AA}$.

Fig. 6: Calculated resolution curve of $\overset{V}{Cl}$ assuming the mean number of photoelectrons is 30. Tails due to γ -rays of energy $\geq 0.75 \text{ Mev}$ and due to hadron interactions in Cl have been included.

Fig. 7: An example of data that will be obtained from a few minute run on a Be target. In simulating this data it was assumed that i) the single particle resolution is as in Fig. 6, ii) that in every inelastic collision there are produced two protons plus a poisson distribution of pions with $\langle n_{\pi^{\pm}} \rangle = 6$.

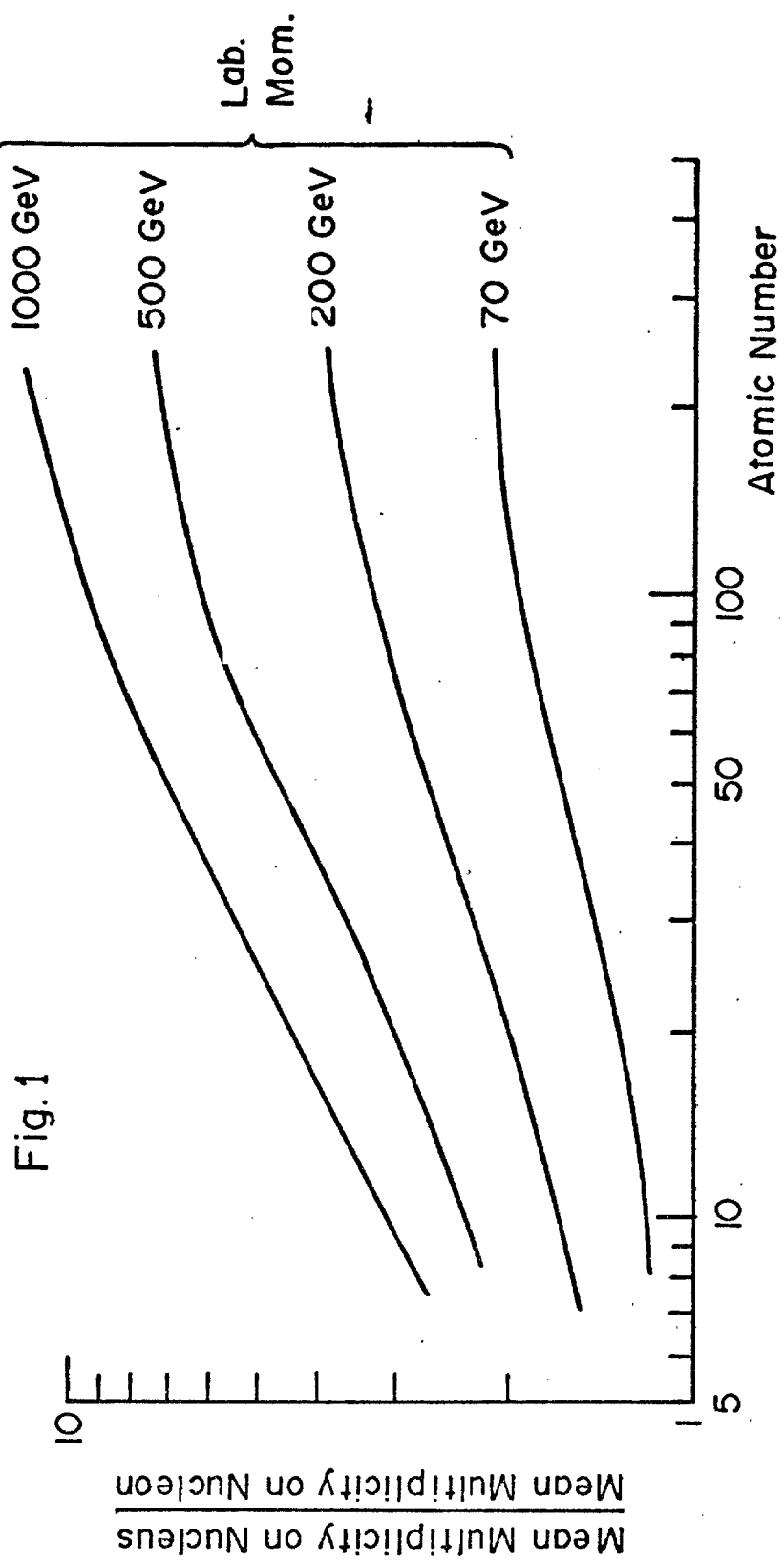
Summary of models, types of experiments, and the predictions made by various models.

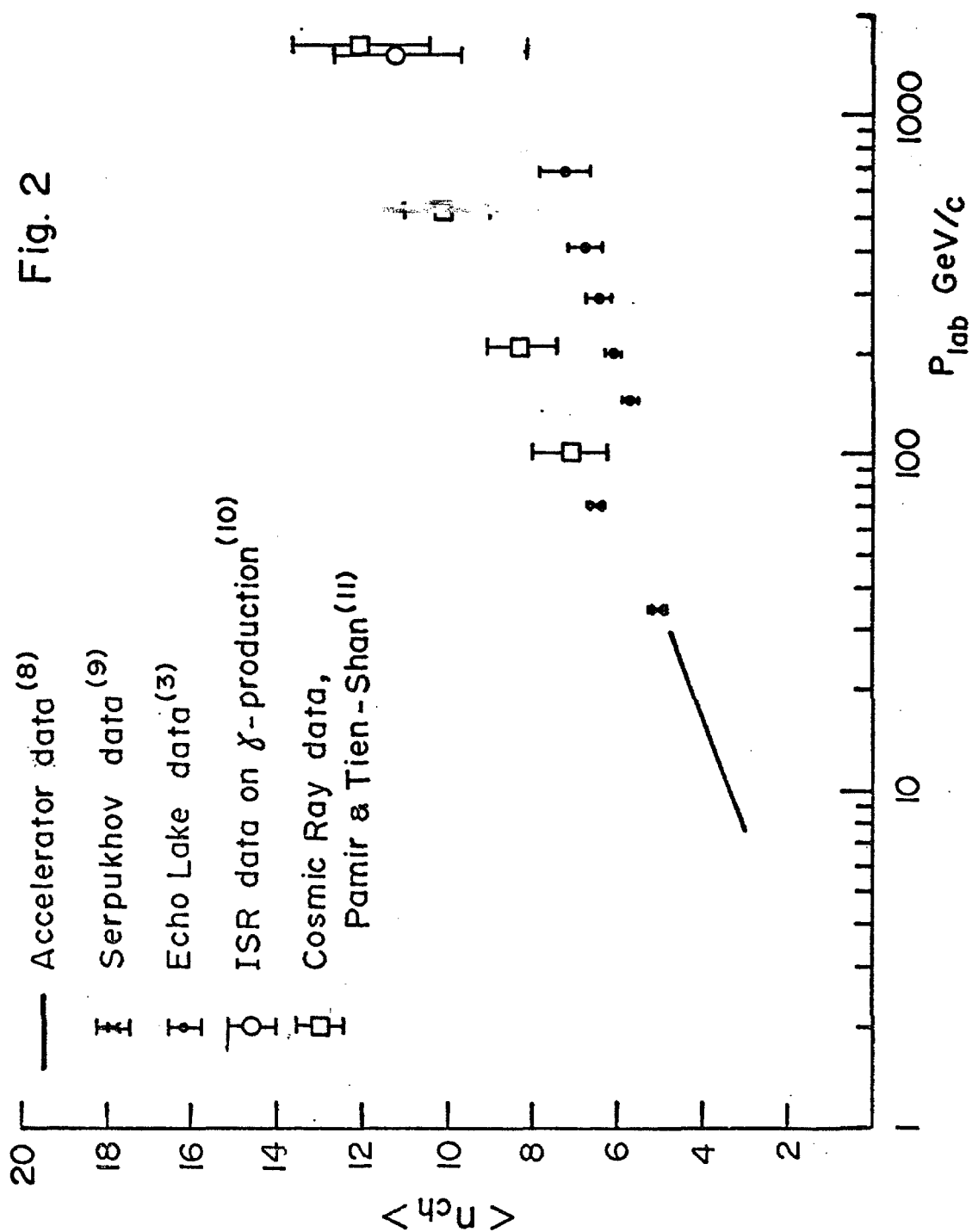
Experiment	Model				Beam energy region	
	(a) Mueller analysis	(b) Multiperipheral	(c) Diffractive fragmentation	(d) Statistical thermodynamics		(e) Cheng-Wu
(1) Average multiplicity $\langle n(E) \rangle$	$\langle n(E) \rangle = a \ln E + b$		No prediction; can accommodate any reasonable behavior	$\langle n \rangle$ grows faster than $\ln E$	$\langle n \rangle \propto s^a, a > 0$ $E > E_p$	
(2) Multiplicity distribution $P(n)$	No prediction	Roughly Poisson	$P(n) \propto n^{-1}$ if $\langle n \rangle \propto \ln E$	No prediction	?	$E > E_p$
Partial cross sections $\sigma_n(E)$	No prediction	$(K \ln s)^{n-1} s^{-K} / (n-2)!$, $K = 2 - 2\alpha_M(0) \approx 1$	Constant	No prediction	?	$E > E_p$
(3) One-particle spectra: limiting fragmentation?	Yes	Yes	Yes	Yes	No; $\rho(q) \propto s^a$	$E > E_f$
(4) One-particle spectra: central plateau?	Yes	Yes	No prediction; can be accommodated	Not in present version; can be accommodated	Yes	$E > E_p$
(5) One-particle spectra: factorization in fragmentation regions	Yes	Yes	?	No prediction	?	$E > E_f$
(6) One-particle spectra: factorization in plateau region	Yes	Yes	No	No prediction	?	$E > E_p$
(7) Two-particle spectra: correlations?	Only short-range correlations, if Regge poles \gg Regge cuts.		No prediction	No prediction	?	$E > E_f$
(8) Diffraction dissociation into high missing mass	$\propto g_{PPP}^2$, triple Pomeron coupling	g_{PPP} small or zero	"Favored"	No prediction	?	
(9) $\sigma_{tot}(E)$	$\sigma \propto \text{const. or } s^{-\epsilon}, \epsilon \ll 1$		Constant	No prediction	$\sigma \propto \ln^2 s$	

TABLE I

Table II

Target Material	A	Z	Coll. length gms/cm^2	Rad. Length gms/cm^2	Approx. Optimum Thickness gms/cm^2	Inelastic Collisions in Target Per 10^6 inc. Particles	Additional Tracks in Cl Due to Showers in Target and Cl E: M. Hadronic
Be	9.01	4	66	63.7	1.3 2.39	3.6×10^4	5% 10%
C	12.01	6	94	42.4	1.3 2.0	2.1×10^4	6% 8%
Al	26.98	13	119	24.0	.70 1.89	1.6×10^4	9% 7%
Cu	63.54	29	152	12.0	.12 1.07	7.0×10^3	10% 5%
Sn	118.7	50	182	8.89	.11 .81	4.5×10^3	10% 5%
Pb	207.2	82	209	6.52	.06 .68	3.3×10^3	11% 5%
U	238.1	92	219	6.13	.04 .75	3.4×10^3	13% 5%
NO TGT. ONLY Cl	≈ 12	≈ 6	≈ 55	≈ 43.4	1 1.05	1.9×10^4	





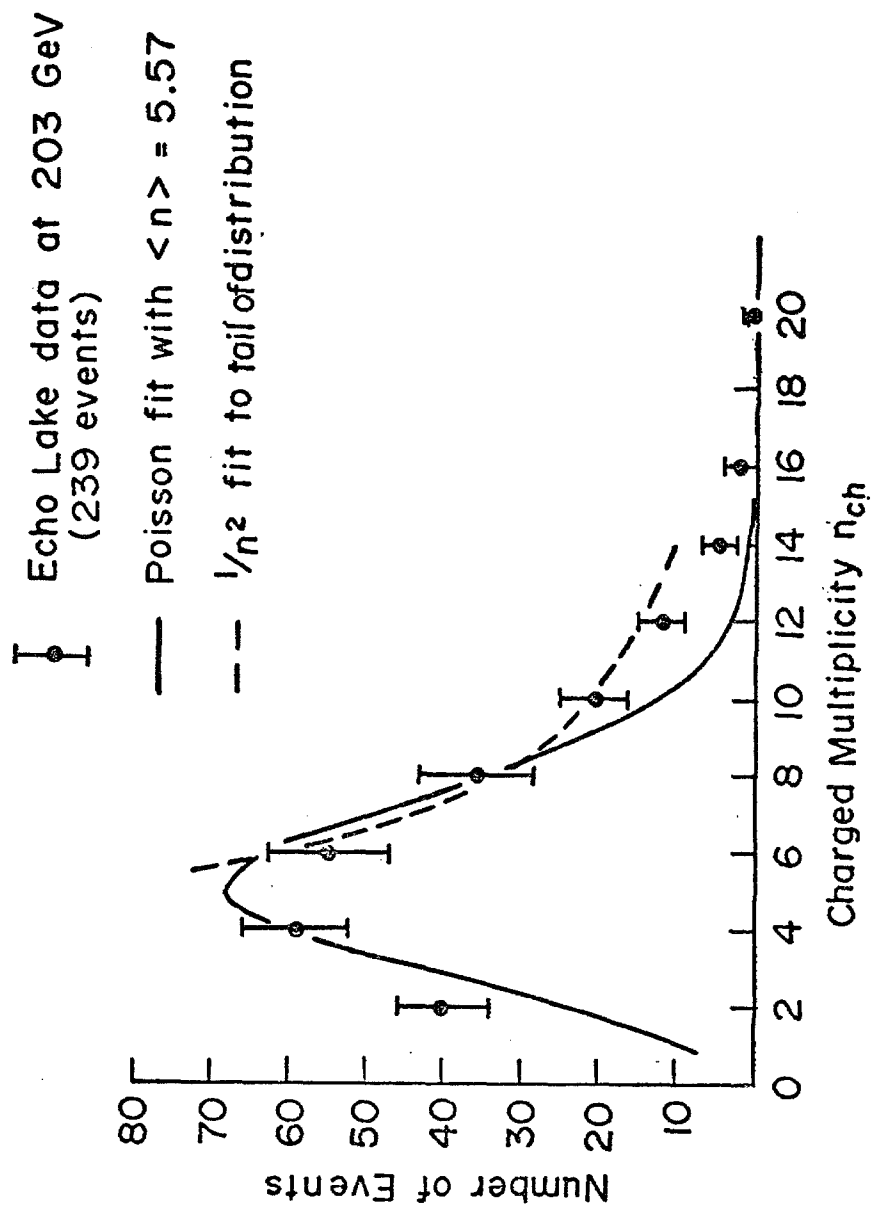


Fig.3

T_1, T_2 & V : Scintillation Counters
 \check{C}_1 & \check{C}_2 : Čerenkov Counters with Polystyrene Radiators
 $\check{C}_3 - \check{C}_6$: Čerenkov Counters with Pilot 425 Radiators

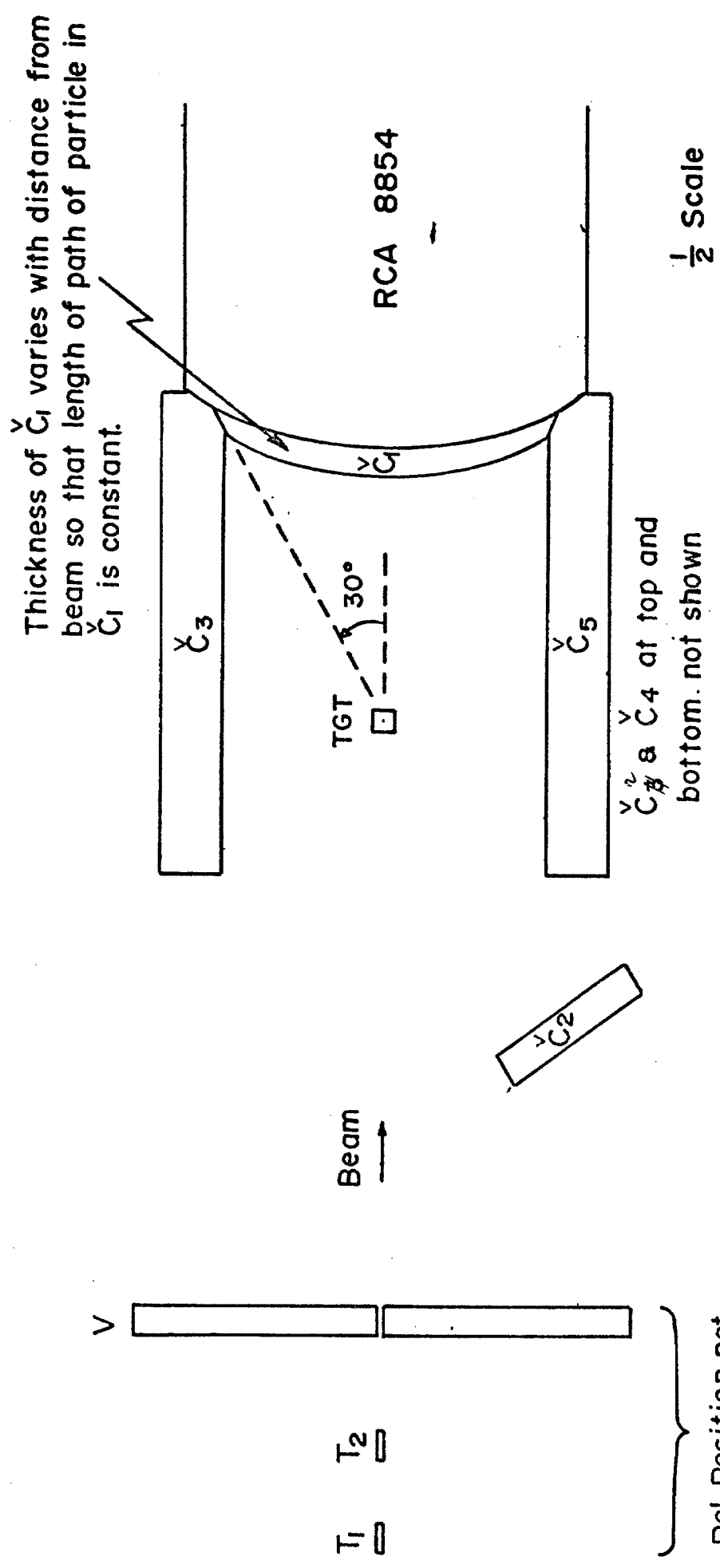


Fig. 4

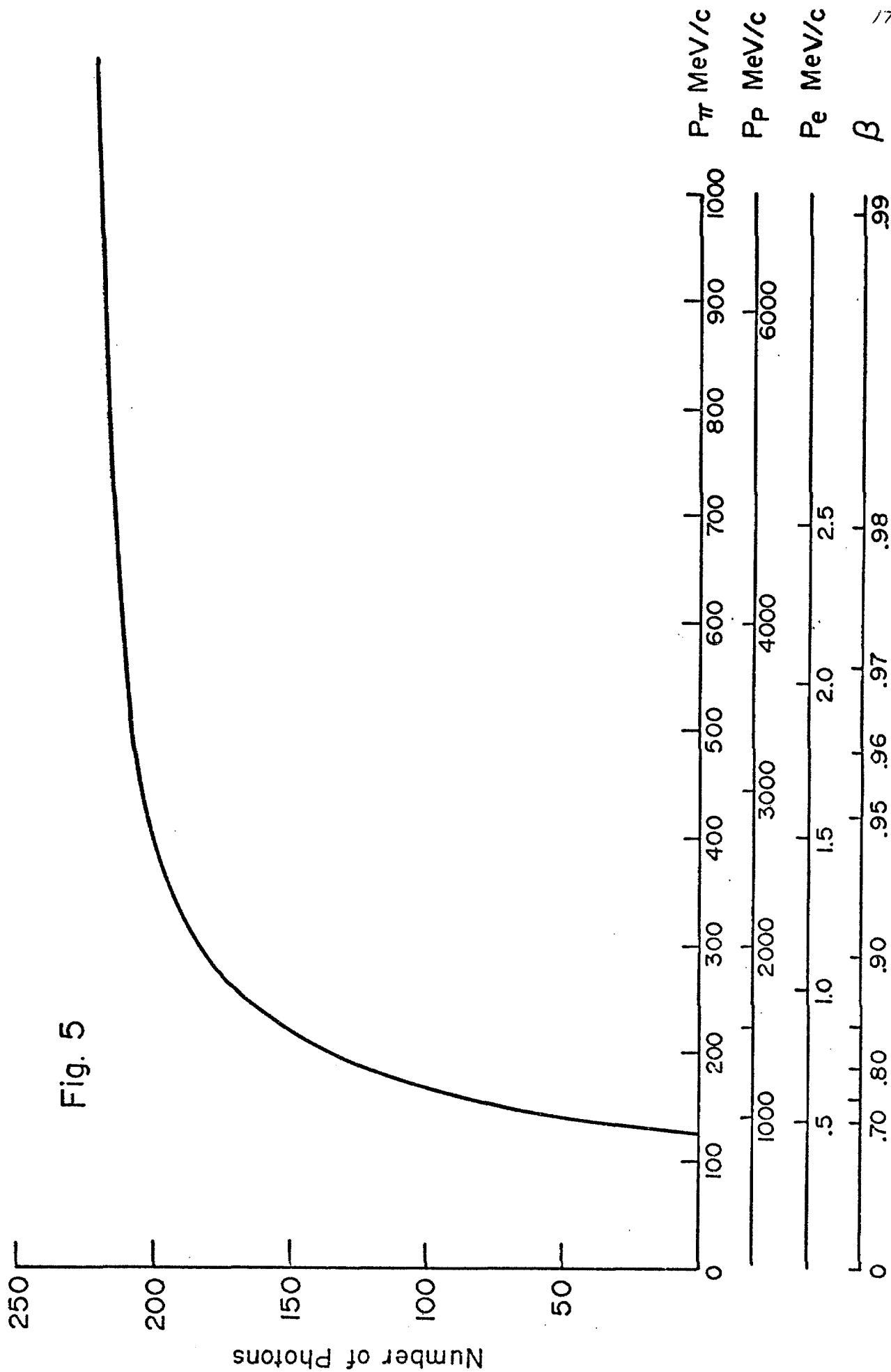


Fig. 6

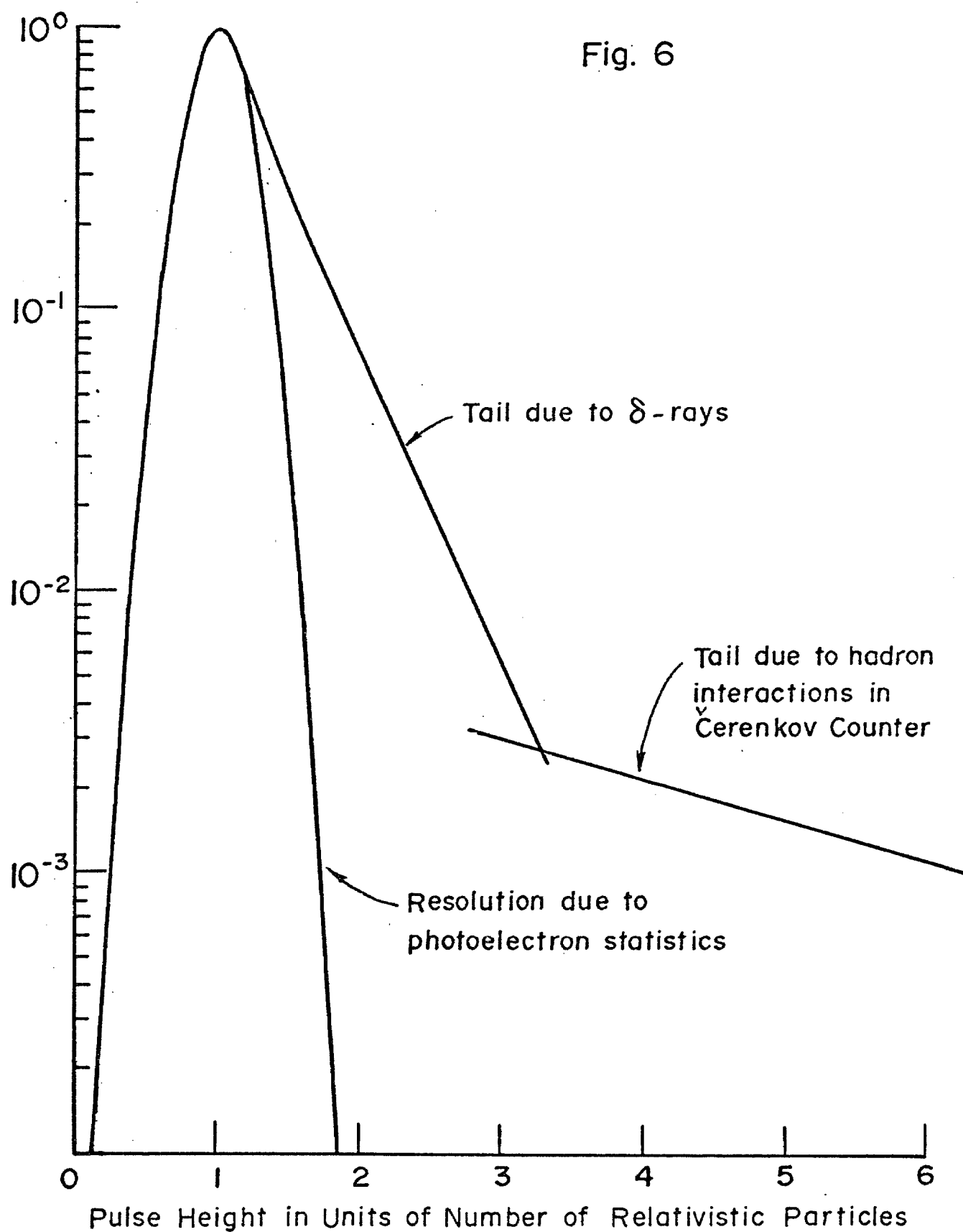
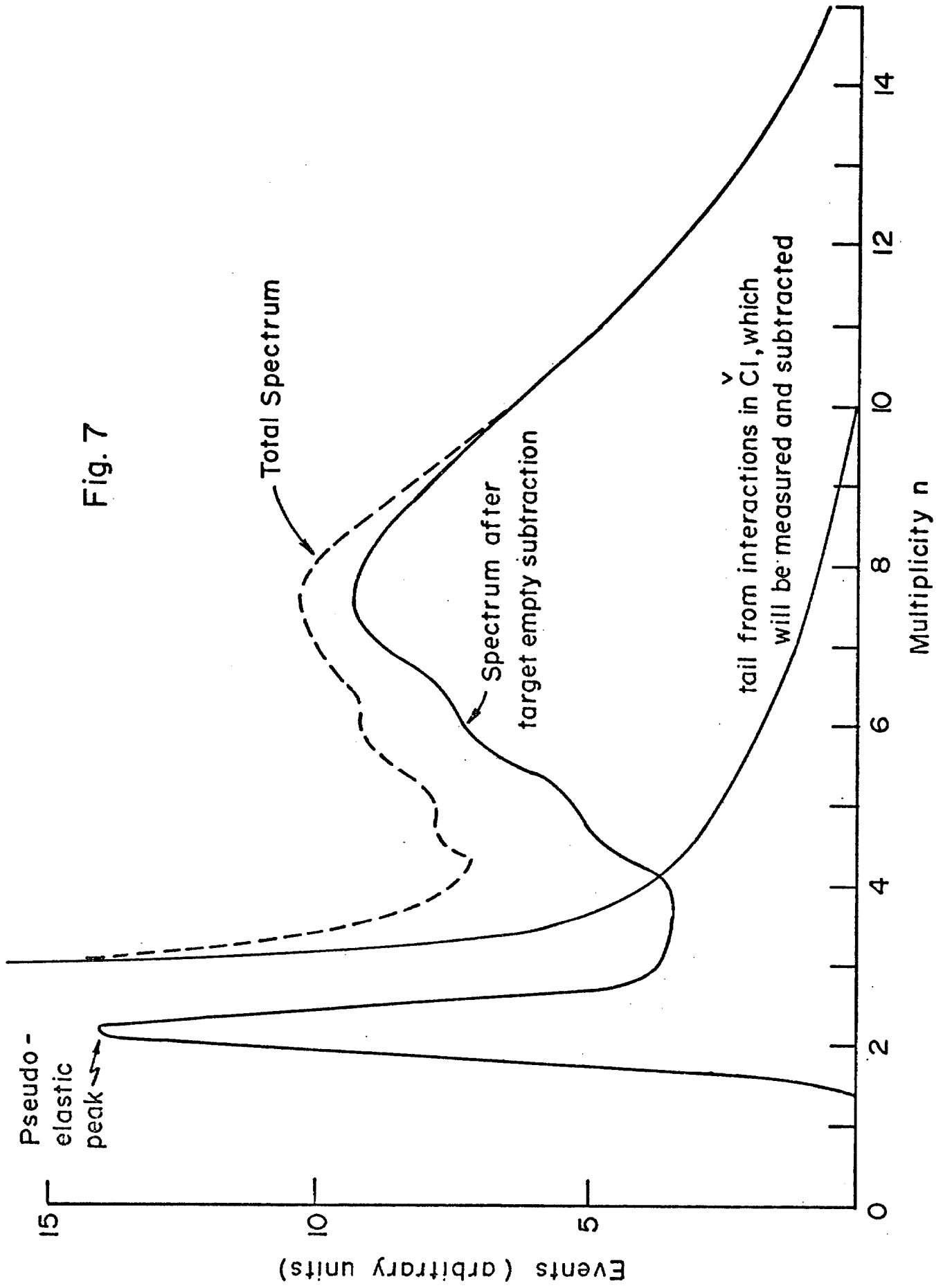


Fig. 7



SUMMARY OF RESULTS OBTAINED AT BNL ON THE PROPERTIES OF
THE DETECTOR PROPOSED FOR NAL EXPERIMENT # 178

W. Busza, J. Elias, S. Redner, M. Sogard

Physics Department and Laboratory for Nuclear Science, MIT

A proposal to study the average multiplicity and multiplicity distributions in hadron-nucleus collisions at high energies was submitted to NAL last July. Following the recommendation of the Program Advisory Committee a preliminary test of the instrumentation was made at the Brookhaven National Laboratory.

Various designs of the crucial forward Čerenkov counter were built and tested in the East Test Beam. The uniformity and resolution of the final design was considerably better than that assumed in the proposal. The overall FWHM resolution of the counter for a relativistic particle was found to be $30/\sqrt{n}\%$, which is adequate for the proposed measurements at NAL.

This report summarizes the results obtained at BNL.

The Scope of the Tests:

The detector proposed for Experiment #178 was designed for counting large numbers of highly relativistic particles produced mainly in a small forward cone. At BNL, for obvious reasons, it was not possible to simulate such conditions and thus we limited ourselves to answering the following question: Is it possible to construct a thin Čerenkov counter ($\approx 1 \text{ gm/cm}^2$) which would:

1) have a very good pulse height resolution for a single highly relativistic ($\beta > .98$) particle passing through any point on the counter. By good resolution we mean FWHM $< 40\%$, suitable for looking at large multiplicity events.

2) not saturate for a light output corresponding to large multiplicities.

3) have an area large enough to detect all particles produced within a forward cone of 30° half angle.

The Čerenkov counter finally built satisfied all the above requirements.

Design of the Čerenkov Counter:

Of all the Čerenkov counters tested, the one illustrated in Fig. 1 has optimum properties. It has a radiator made of UVT plexiglass in the shape of a plano-concave lens. The curved shape

compensates for a decrease in pulse height as the angle of the particle goes off axis. The RCA4525 photomultiplier has a plane, 5" diameter, bialkali photocathode and a venetian blind dynode structure. It was interesting to observe that the uniformity of response of this photomultiplier was significantly superior to that of the more expensive photomultipliers such as RCA4522. The only disadvantage of the RCA4525, not important as far as the proposed experiment is concerned, is the slow rise time, ≈ 17 nsec.

Pulse Height Resolution:

Figs. 2 and 3 show the pulse height resolution of the Čerenkov counter when a single particle (9 GeV proton) passes through the center of the counter. The following should be noted:

- 1) The FWHM resolution, including the δ -ray tail, is 25%. This is considerably better than the 40% assumed in the proposal.
- 2) The δ -ray and hadron tails are as anticipated in the original proposal.
- 3) The fact that the beam passes through the dynode structure causes no problems.

Fig. 4 illustrates how the pulse height varies across the surface of the counter. The maximum variation between any two points is 14%.

Folding these two measurements together we obtain an overall resolution of 29%.

To check this result, half a collision length of carbon was placed in the 9 GeV proton beam in front of the \check{C} counter. Between the carbon target and the \check{C} counter a $\frac{dE}{dX}$ counter was inserted. The \check{C} counter was gated with the $\frac{dE}{dX}$ counter. Fig. 5 shows the spectrum obtained in the \check{C} counter for $\frac{dE}{dX}$ set to twice minimum ionizing. The presence of the first peak is clear indication that the spectrum contains, in addition to relativistic particles, particles of low velocity. The width of the second peak gives an upper limit of 34% on the overall resolution of the detector. To obtain a better estimate we fitted both the peaks in Fig. 5 with a Gaussian plus a δ -ray tail and obtained a resolution of 28%, consistent with the resolution concluded from measurements of the variation of pulse height across the area of the counter.

In Fig. 6 we show the spectrum when the $\frac{dE}{dX}$ counter was set to four times minimum ionizing. The figure is shown to demonstrate that the \check{C} counter can differentiate different multiplicities. The reason why different multiplicities appear is that some particles that contribute to $\frac{dE}{dX}$ in the scintillation counter do not have sufficient velocity to give \check{C} erenkov light.

Saturation of the Photomultiplier:

The output from the photomultiplier was approximately 50 mv for one particle passing through the radiator. Light pulser tests indicated a linear response up to outputs of > 2.5 volts, which corresponds to > 50 particles in the counter.

Monte Carlo Simulation of Data:

We have simulated data that will be obtained at NAL, for simplicity the resolution was assumed to be a pure Gaussian with a width of $30/\sqrt{n}\%$. A typical spectrum that will be obtained after 10^7 incident protons (\approx few minutes) is illustrated in Fig. 7.

CONCLUSION:

A \checkmark Čerenkov counter has been built which is suitable for the proposed experiment. The overall resolution is significantly better than that which was assumed in the proposal. The FWHM resolution of the counter for n particles is $30/\sqrt{n}\%$.

In Fig. 8 we summarize the present knowledge of multiplicity distributions in proton-proton collisions up to 300 GeV. The resolution achieved indicates that the proposed technique should be capable of reproducing these measurements and even extending them to higher values of n in hadron-nucleus interactions. In particular there should be no difficulty in obtaining detailed data on the variation of the mean charged multiplicity with nuclear size.

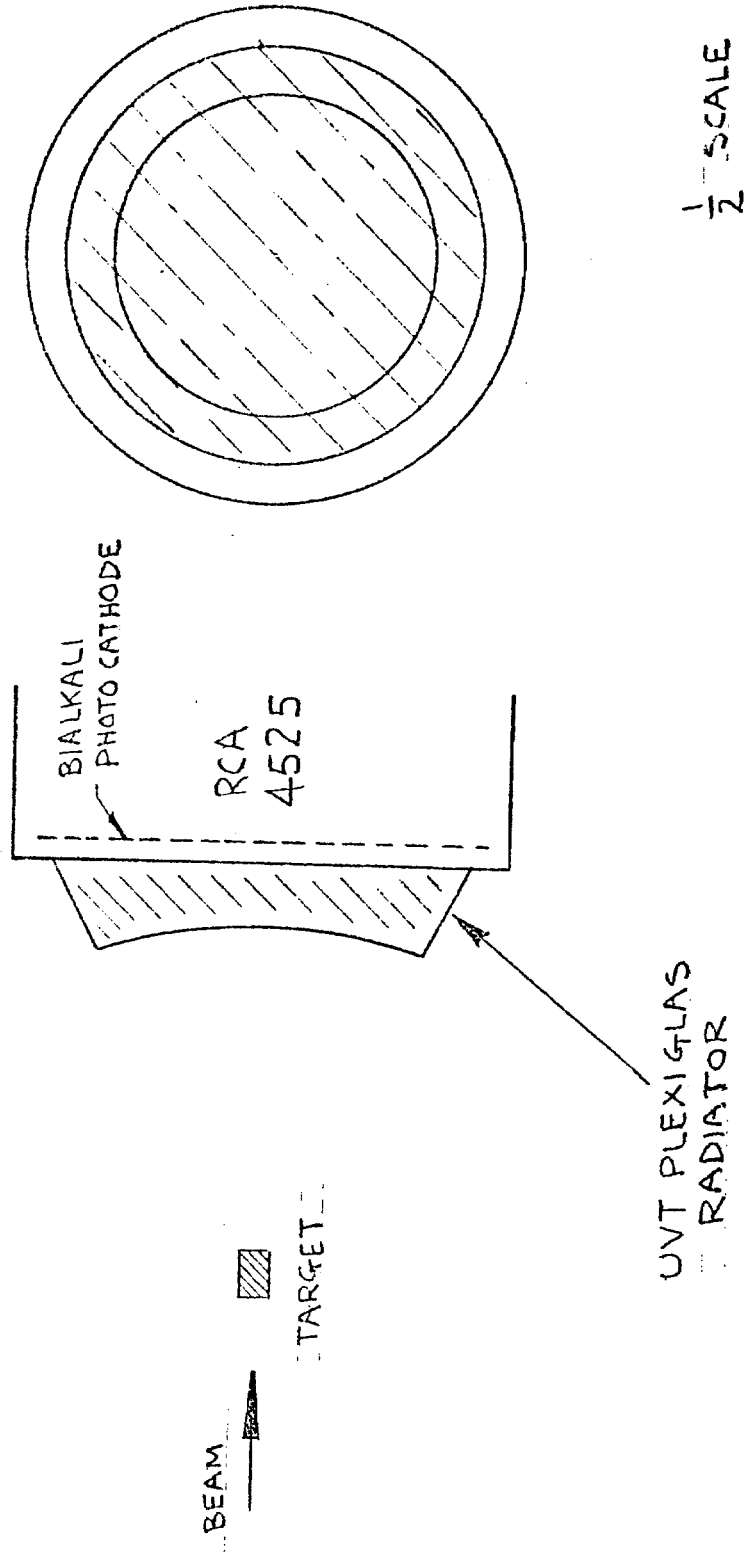


FIG. 1 ČERENKOV COUNTER

FIG. 2 PULSE HEIGHT SPECTRUM FOR ONE PARTICLE
PASSING THROUGH CENTER OF \bar{c} COUNTER

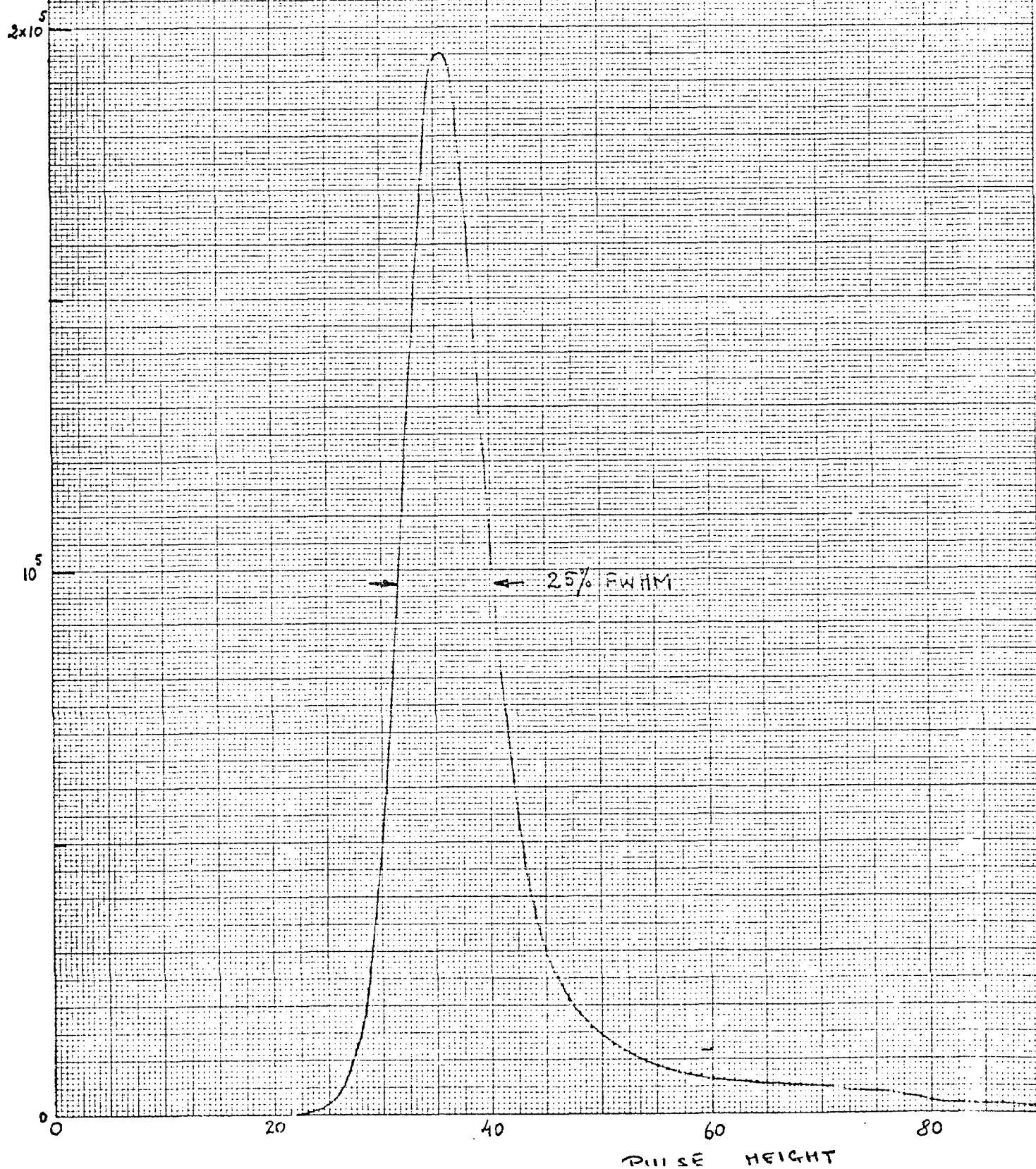


FIG. 3 PULSE HEIGHT SPECTRUM FOR ONE PARTICLE
PASSING THROUGH CENTER OF C COUNTER

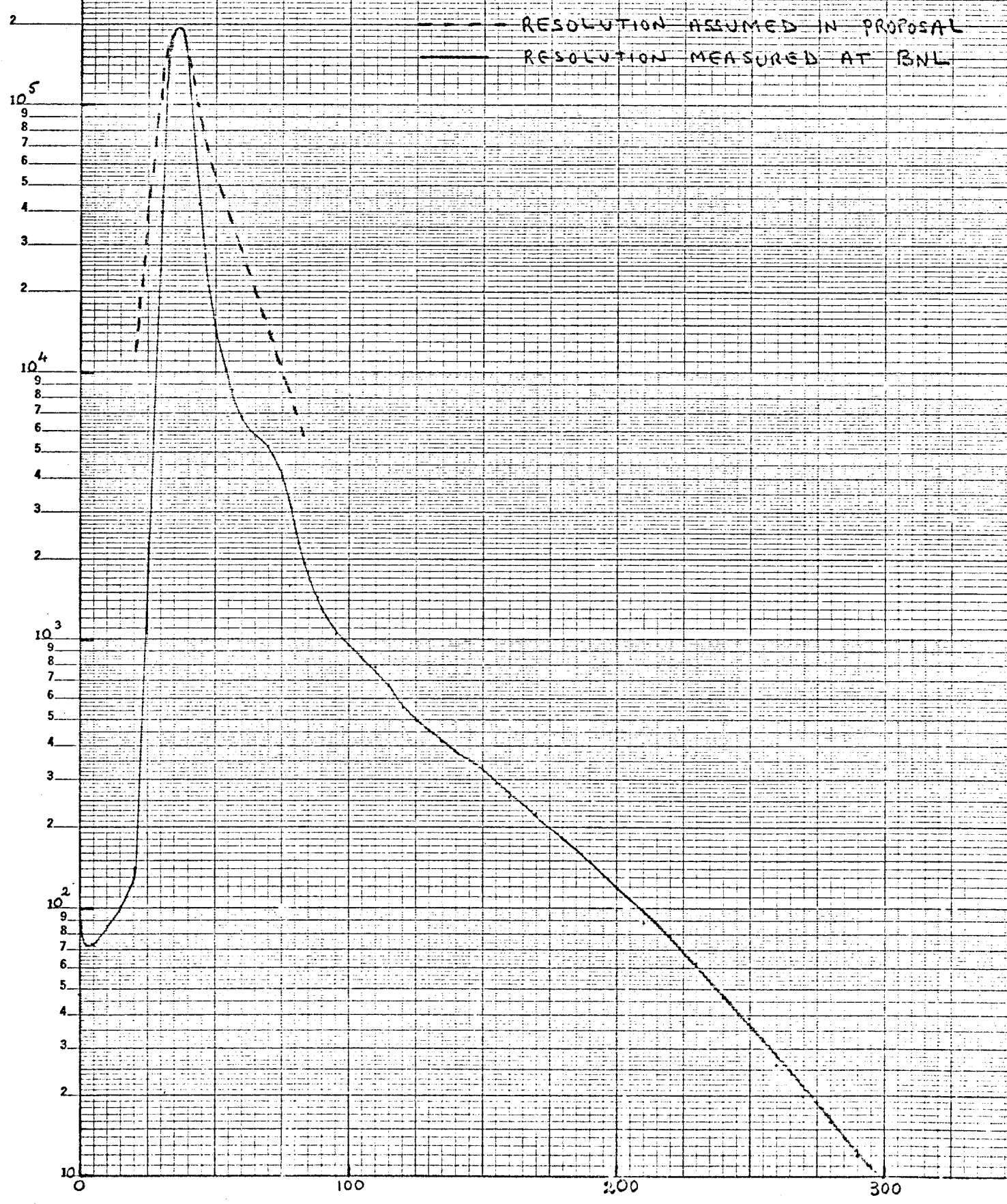
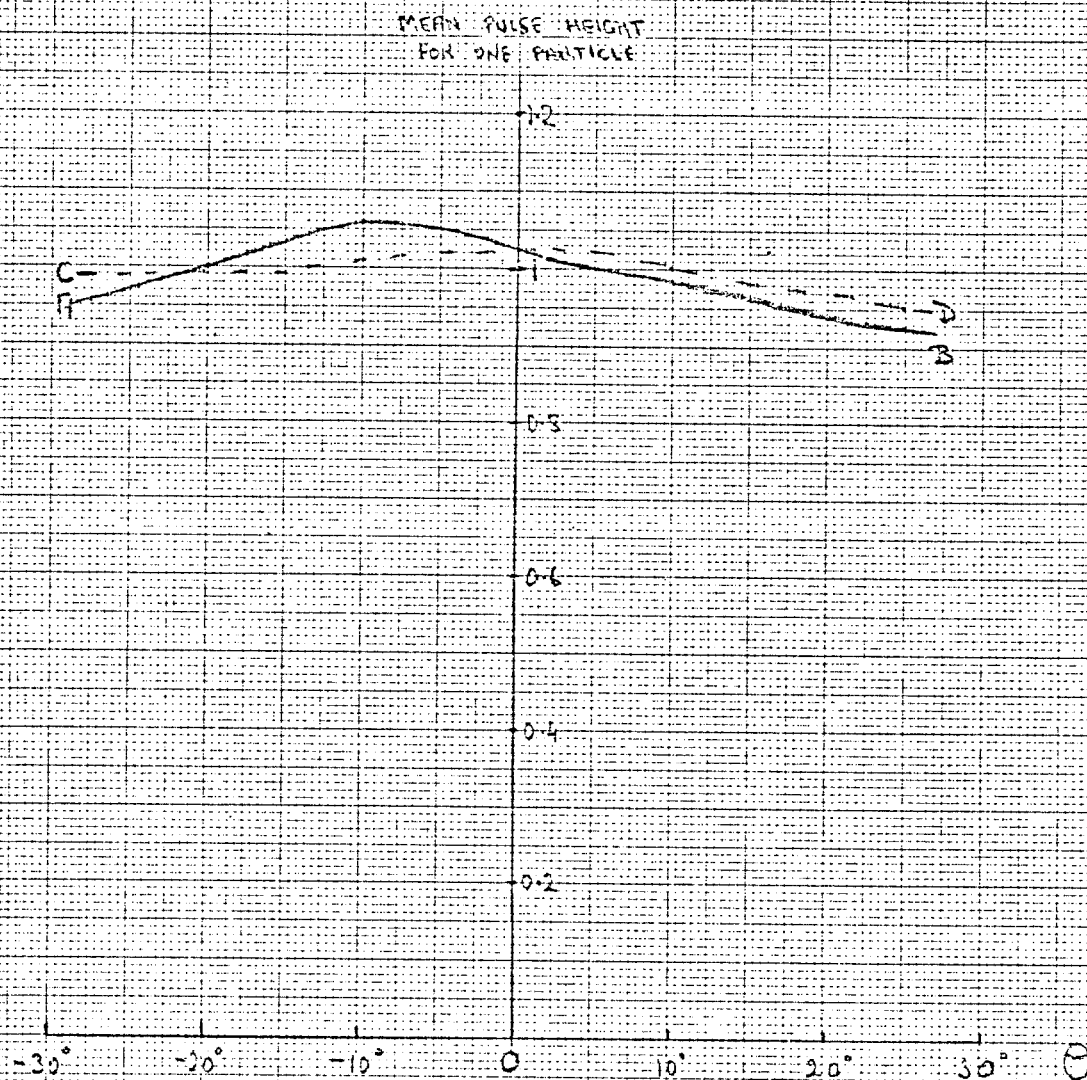


FIG. 4

UNIFORMITY OF RESPONSE OF ČERENKOV COUNTER ACROSS AREA OF PHOTOCATHODE



9 Gev. proton
beam
→

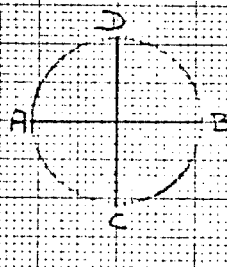
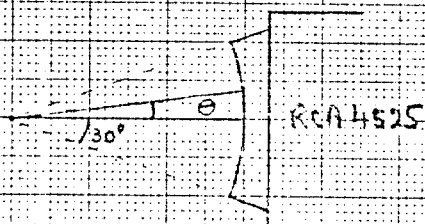


FIG. 5 PULSE HEIGHT SPECTRUM FOR EVENTS SATISFYING $\frac{dE}{dX} = 2 \times 10^{11} \text{ eV/g}$

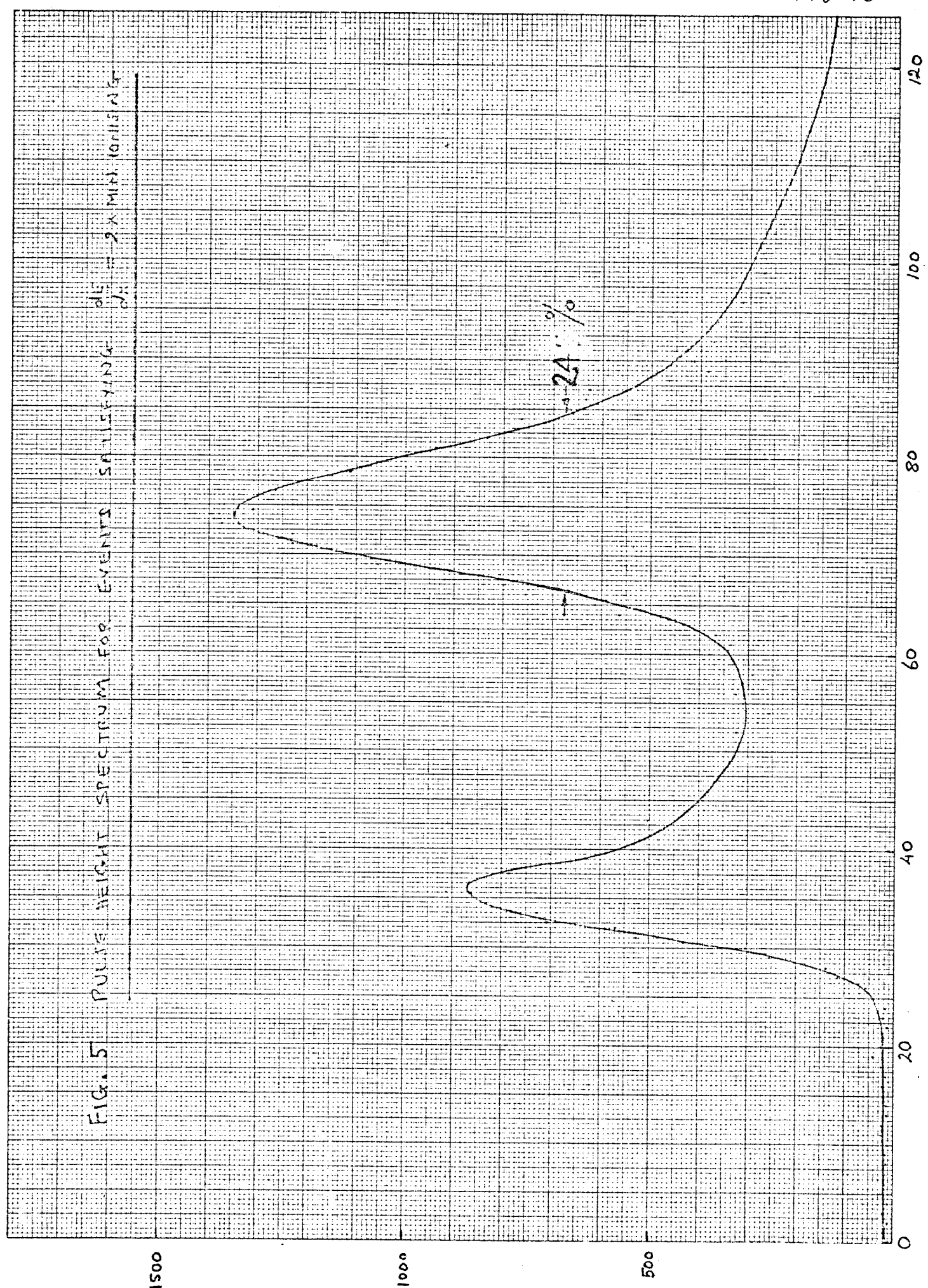
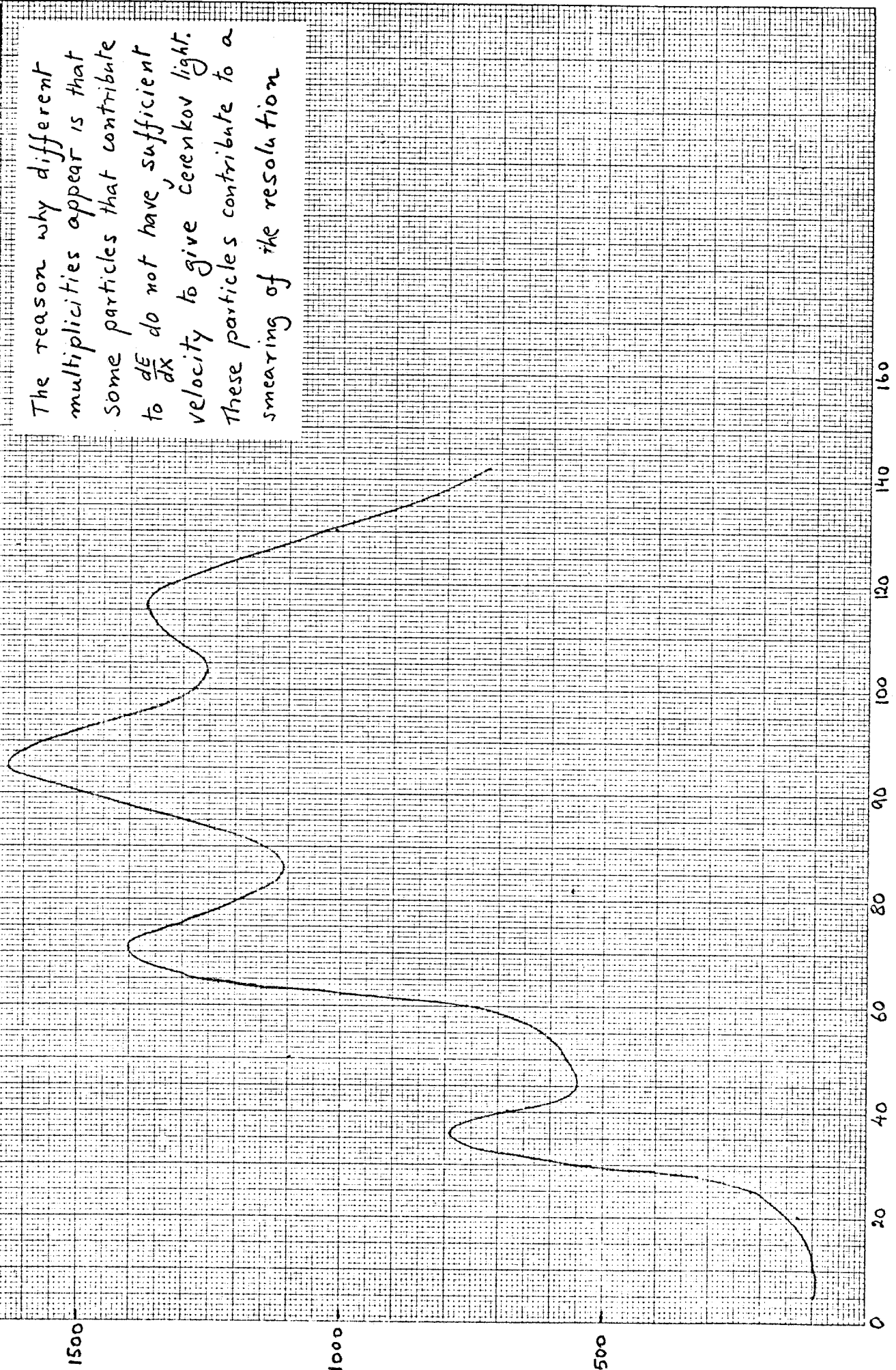


FIG. 6. PULSE HEIGHT SPECTRUM FOR EVENTS SATISFYING $\frac{dE}{dX} = 4 \times \text{MIN. IONISING}$



The reason why different multiplicities appear is that some particles that contribute to $\frac{dE}{dX}$ do not have sufficient velocity to give Cerenkov light. These particles contribute to a smearing of the resolution

FIG. 7 MONTE CARLO SIMULATED RESULT
 (FEW MINUTES OF DATA TAKING)

THE HISTOGRAM IS THE MODEL
 USED FOR THE DISTRIBUTION FUNCTION

THE CURVE SHOWS HOW THE
 DISTRIBUTION FUNCTION
 WILL BE SMEARED BECAUSE
 OF THE EXPECTED RESOLUTION
 OF THE COUNTER. A GAUSSIAN
 OF $FWHM = 30/\sqrt{n} \%$ WAS USED
 IN GENERATING THIS SPECTRUM.

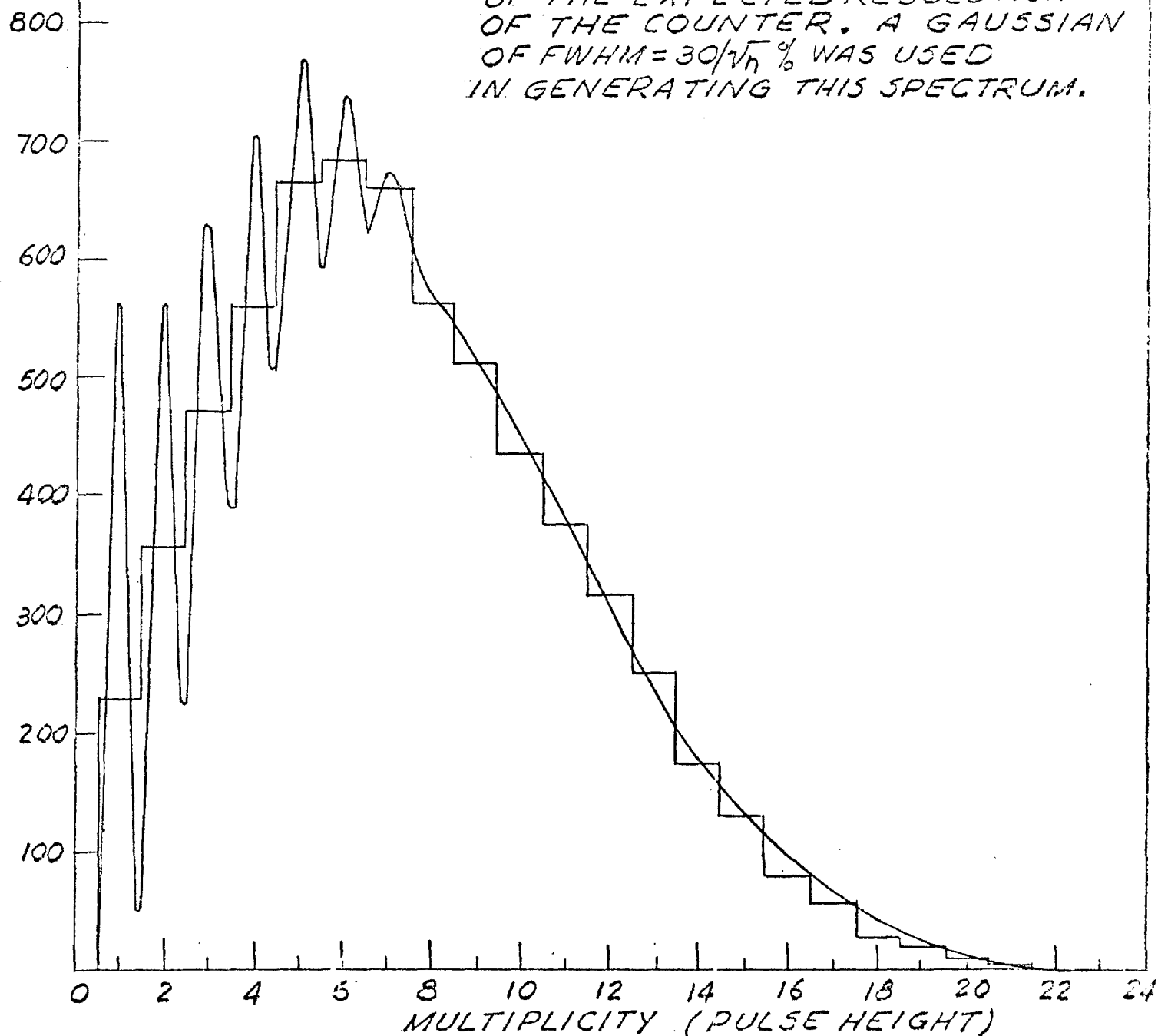
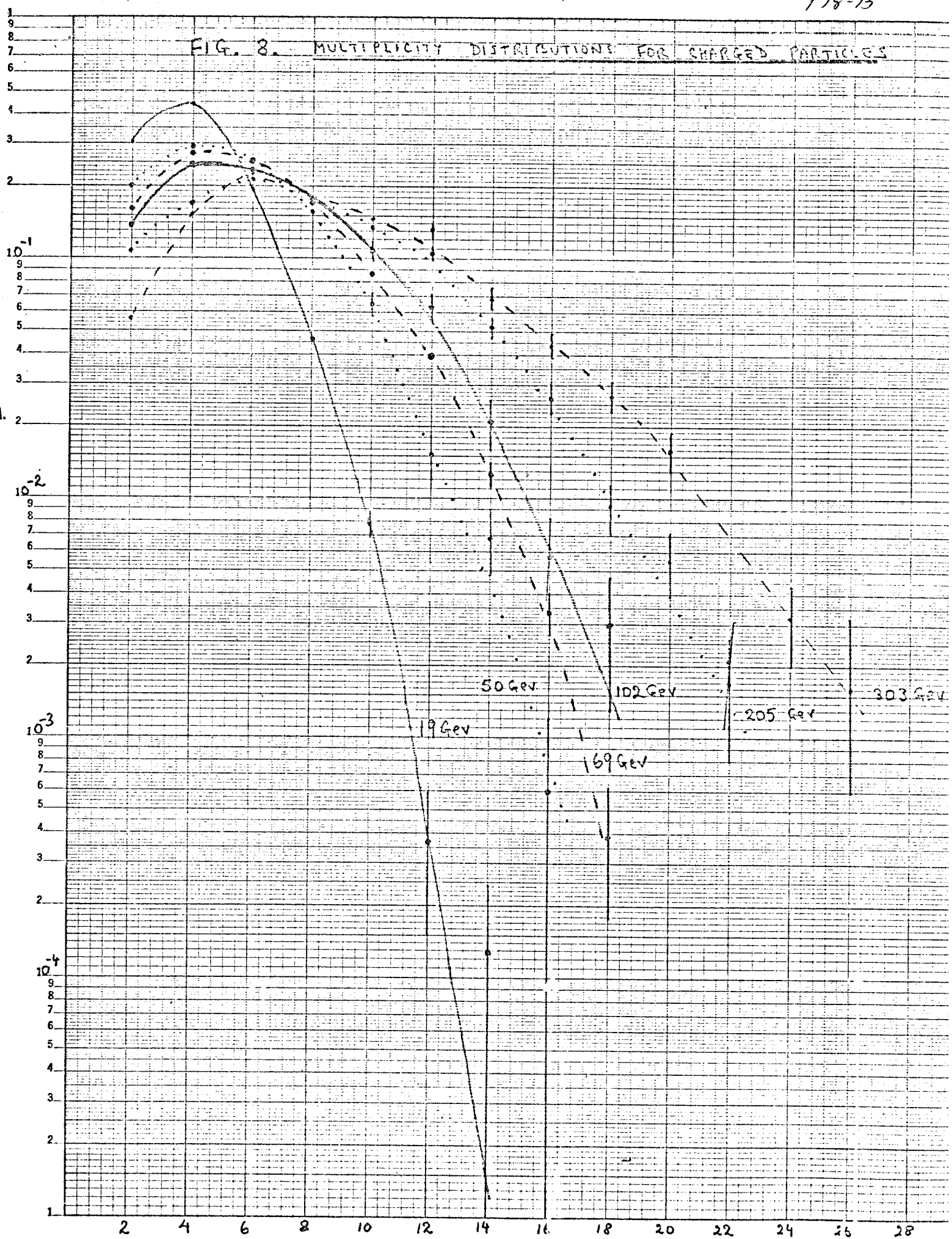


FIG. 8. MULTIPLICITY DISTRIBUTIONS FOR CHARGED PARTICLES

 $\sigma_{\text{incl.}}$ 

MULTIPLICITY